

Chapter 2

Moment Tensor Solution and Physical Parameters of Selected Recent Seismic Events at Rudna Copper Mine

Grzegorz Lizurek and Paweł Wiejacz

Abstract The Lubin Copper Basin is a source of induced seismic events of considerable size. The paper presents the source mechanism study of fifty seismic events from Rudna Copper Mine that occurred in 2007. The energies of studied seismic events were greater than 10^5 J. Focal mechanisms for those events have been calculated with seismic moment tensor inversion method using FOCI computer software. The calculations were made using L1 and L2 norms. Final results are presented for L1 norm due to its lower sensitivity to possible errors. Spectral analysis of P and S waves was also performed. The analysis shows that typical focal radius is of about 200 m.

2.1 Introduction

Seismic moment tensor solutions and physical parameters of seismic events in mines could be an extension of seismic event location and energy calculation routines in mines. The information about focal mechanisms and source parameters can be used in mining engineering together with the focal coordinates and energy of tremors that are used now. Estimation of the fault planes, focal radii and their spatial analysis done periodically can point out if any of direction in space is more often observed than others. If so, then it may prove useful to try to connect it to geological or mining features such as an old fault in or near mine region (re) activated during mining processes or new fault formation, the direction of caving works or any prevailing direction of cracks or layering in the rockmass. The knowledge of mechanisms of events and focal radius can be also taken into account in blasting procedure used in mining practice of stress release and extraction of

G. Lizurek (✉) • P. Wiejacz

Institute of Geophysics, Polish Academy of Sciences, Księcia Janusza 64, 01-452 Warszawa, Poland

e-mail: lizurek@igf.edu.pl

deposits. For the purpose of this study, we have selected 50 seismic events induced at Rudna Copper Mine in the second half of 2007. For those events we have calculated source parameters and source mechanisms with seismic moment tensor inversion method.

2.2 Rudna Copper Mine: Network and Data

Rudna Copper Mine is located in the Legnica-Glogow (Lubin) Copper District, Southwestern Poland. Seismograms of 50 mine induced events in 2007 of energy higher than 10^5 J recorded by Rudna Copper Mine seismological network (Fig. 2.1) were analyzed. Data selected for our study was provided by Rudna Copper Mine.

Spectral analysis of P and S waves, physical properties of foci and moment tensor solutions of all selected events were determined. Coordinates of foci and origin time were provided by Rudna Copper Mine. Due to huge errors of the Z coordinate estimation in near-plain geometry of mine network, event depth is commonly fixed at the excavation level. The Rudna Copper Mine local network is composed of 32 vertical seismometers at mining level, except of two sensors placed in elevator shafts. However, the sensors in shafts were very rarely used, because of the noise coming from the shafts. The depth range of seismometers location is from 300 down to 1,000 m below surface.

During the period of the study the most active mining divisions had about 15 events of energy higher than 10^5 J. Distribution of events in mine subdivisions according to their energy is shown in Fig. 2.2.

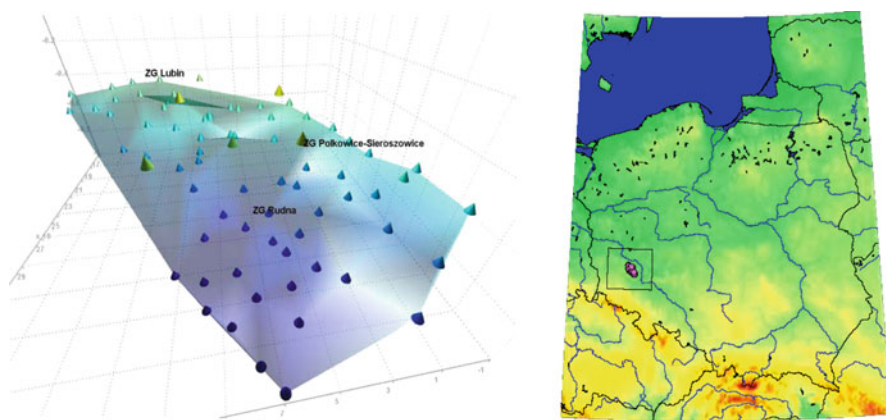


Fig. 2.1 The Rudna Copper Mine seismic network along with networks of neighbouring mines. *Right:* location of the area on the map of Poland

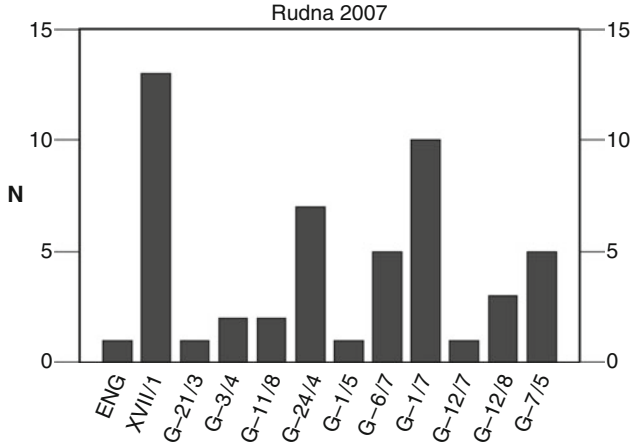


Fig. 2.2 Histogram of number of events in mine subdivisions

2.3 Spectral and Physical Parameters of Events

The basis of the study are ground motion spectra that had been obtained by integration of velocity seismograms. The relevant parts of seismograms of P and S waves were selected manually, and then transformed by Fast Fourier Transformation (FFT). Resulting amplitude spectra were corrected for attenuation effects with $Q = 400$ and 200 , respectively, for P and S waves. For further calculations we set velocities of P and S waves at $V_p = 5,700$ m/s and $V_s = 3,300$ m/s. Far field displacement spectra were approximated on logarithmic scale. The two asymptotes were calculated using integrals of squared displacement and velocities of ground motion. This has allowed to estimate the spectral plateau, corner frequency and energy flux in observation point for every spectrum of P and S waves. Next, energies of P and S waves were calculated from the energy flux in far field displacement.

The observed S wave to P wave energy ratio is within the range from 6 to 70, but as it is shown in Fig. 2.3 the ratio value near 10 is typical to most of the events. Higher values of S to P wave energy ratio (higher than 20) indicate that in the focal mechanism the DC (Double-Couple) forces are dominant. The value of the ratio lower than 20 indicates that other components of the mechanism solution are also present.

Average seismic moment M_0 , according to Aki and Richards (1980), $M_0 = \frac{4\pi\rho_0 c_0^3 R \Omega_0}{F_C R_C S_C}$, from all channels recorded for particular events was estimated with spectral plateau of P and S waves frequency spectra:

$$\Omega_0 = 2 \left(\frac{K^3}{J} \right)^{\frac{1}{4}},$$

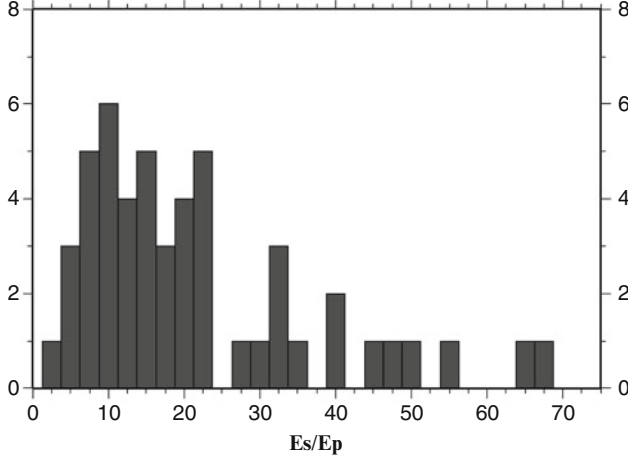


Fig. 2.3 Es vs. Ep ratio for analyzed events from Rudna mine

where J and K are as follows:

$$\begin{aligned}
 J &= 2 \int_0^{\infty} |V(\omega)|^2 df = 2 \int_0^{\infty} \omega |U(\omega)|^2 df \\
 &= \frac{2}{3} [\Omega_0 \omega_1]^2 f_1 + 2 \int_{f_1}^{f_2} \omega |U(\omega)|^2 df + 2 |\omega_2 U(\omega_2)|^2 f_2 \\
 K &= 2 \int_0^{\infty} |U(\omega)|^2 df \\
 &= 2 |U(\omega_1)|^2 f_1 + 2 \int_{f_1}^{f_2} |U(\omega)|^2 df + \frac{2}{3} |U(\omega_2)|^2 f_2 \\
 K &= \frac{1}{4} \Omega_0^2 (2\pi f_C)
 \end{aligned}$$

In these equations, $U(\omega)$ is the far-field displacement in the frequency domain, $V(\omega)$ is the far-field ground velocity in the frequency domain, f_1, f_2 are limits of the bandwidth of seismic instruments, ρ_0 is the density of source material, c_0 is the P or S-wave velocity at the source, R is the source-receiver distance, F_c accounts for radiation of P or S-waves, R_c accounts for the free surface amplification of either P or S-waves amplitudes, and S_c is the site correction for either P or S-waves (Snoke 1987; Andrews 1986).

Then the magnitude was calculated from the equation (Hanks and Kanamori 1979):

$$M_L = \frac{2}{3} \log M_0 - 6.05$$

The magnitude distribution of the events and seismic moment histogram are presented in Figs. 2.4 and 2.5, respectively. The analyzed events are characterized by narrow range of seismic moment values -2.1×10^{12} – 4.2×10^{14} , corresponding to magnitudes M from 2.2 to 3.7. Most of the tremors had smaller magnitudes (less than 2.8).

The focal radius R has been calculated using the formula of Madariaga (1976):

$$r_0 = \frac{K_C \beta_0}{2\pi f_C},$$

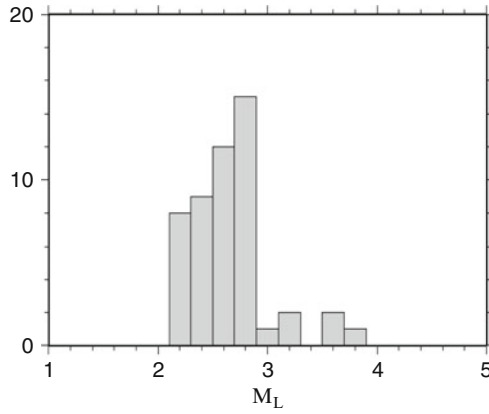


Fig. 2.4 Number of events of different magnitudes

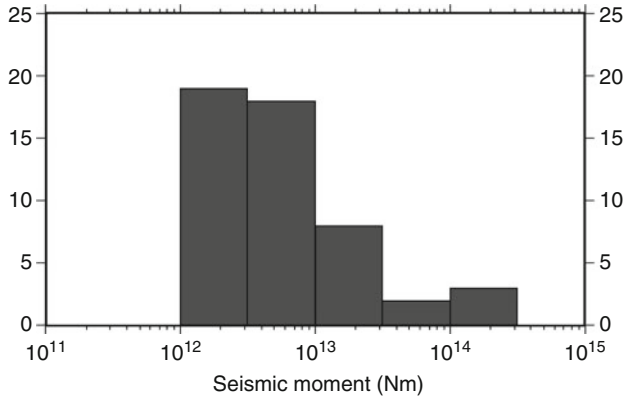


Fig. 2.5 Seismic moment histogram

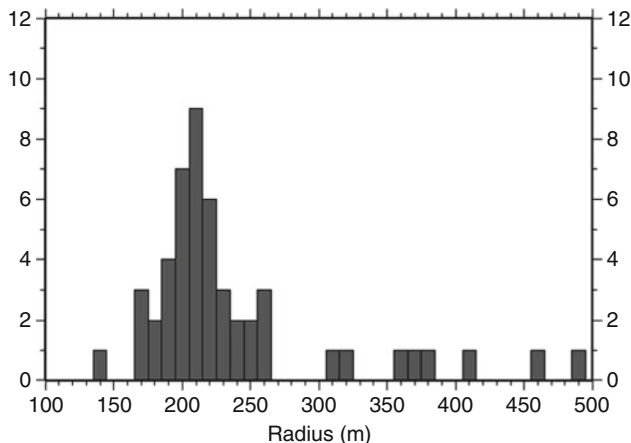


Fig. 2.6 Distribution of focal radii of studied events

where β_0 is the S-wave velocity in the source area, and K_C is a constant depending on the source model.

The results shown in Fig. 2.6 are mean values of radius calculated from all channels for a given event. The dominant value of focal radius appears to be 200 m, but the range of estimated radii is between 135 and 488 m. Therefore, it can be assumed that radius size region around the focus is weakened by the rupture cracks that evolved during the seismic event. The size of focal area is considerable as compared to the gallery size in the mine.

2.4 Focal Mechanism: Moment Tensor Solutions

Focal mechanisms were calculated by moment tensor inversion technique with use of first arrivals, amplitudes and signs of the arrivals. Norms L1 and L2 were applied to calculations; the depth of focus was assumed as an excavation level. All analyses and calculations were done with FOCI software.

Three types of seismic moment tensor have been calculated for each event: full moment tensor, trace null tensor and double couple (DC) moment tensor. The full moment tensor gives no mathematical constraints on the solution, however it is most prone to data errors, especially in case of poor sensors geometry in underground mines. The full tensor can be decomposed into volume change, linear compression/dilatation and shear motion. The trace null tensor is constrained by no net volume change at source. The third tensor is a pure DC, assuming the shearing motion at the focus only (Wiejacz 1991).

Although all types of solutions were calculated for every studied event, the quality of the solution (Fig. 2.7) differed due to numerical errors of solution and compatibility of direction of first arrival signs of the P wave. In case of events that

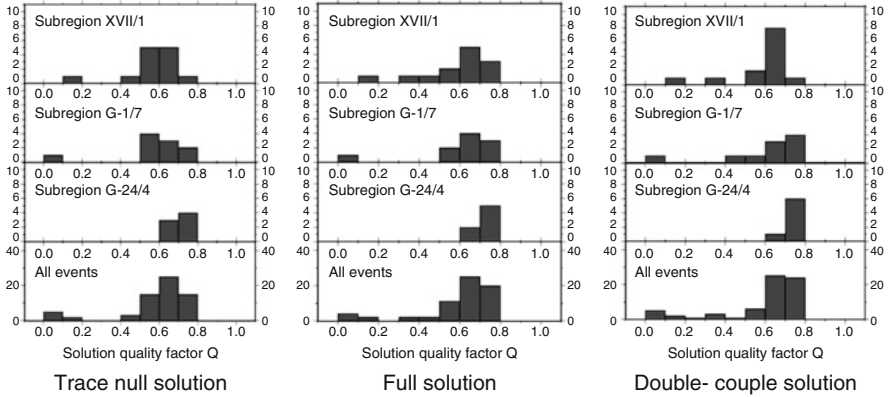


Fig. 2.7 Histograms of solution quality for trace null, full and DC solutions

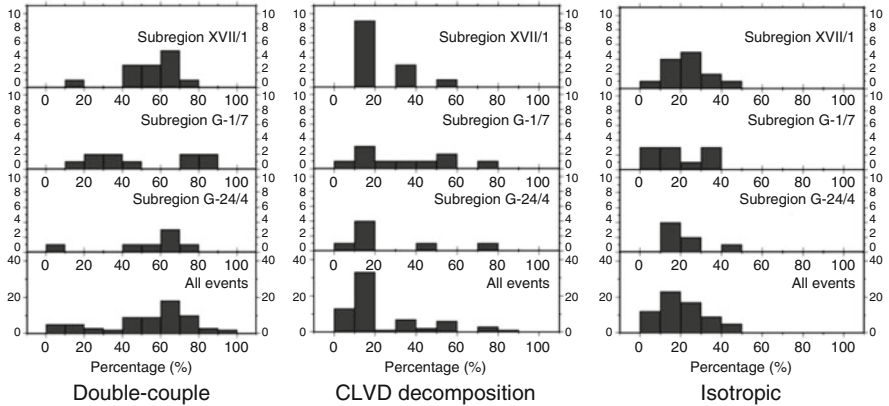


Fig. 2.8 Histograms of decomposition components for full tensor moment solutions

had taken place near borders of the local seismic network, the sensor distribution could have a negative influence on the quality of inversion of moment tensor. This is shown in Fig. 2.7 where quality factors are mostly between 0.6 and 0.8 with only a few events of poor quality (below 0.5).

Most of events had predominant DC component. A significant number of events had also some CLVD and isotropic components involved (Fig. 2.8). We did not observe any dominant fault plane for all events as well as for subregions analyzed separately.

The final results are presented for L1 norm solution. Although the Q factors for L2 norm often are higher, L1 norm solutions appeared to be more coherent for the studied events. Quality of solutions obtained with the use of norm L2 had a higher amplitude between the best and the worst cases than in the case of Q values for L1 norm (Fig. 2.7).

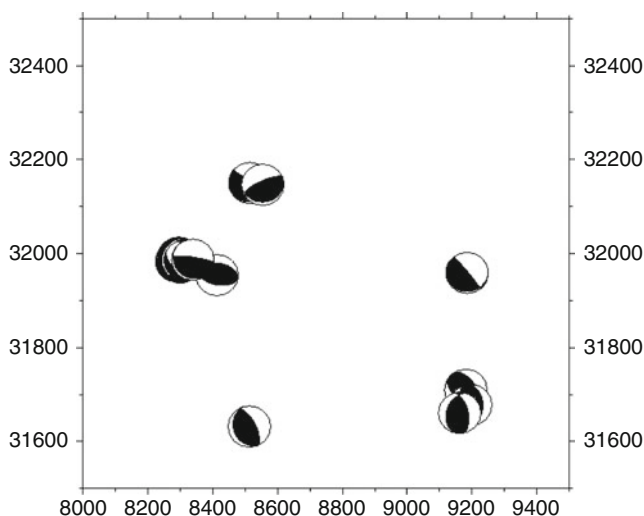


Fig. 2.9 DC solutions of moment tensor inversion for XVII/1 mining subregion of Rudna Copper Mine

2.5 Summary

We have analyzed 50 events from Rudna Copper Mine induced in the second half of 2007 obtaining spectral and physical parameters and focal mechanisms for every event. Radii of foci indicating sizes of focal areas were between 135 and 488 m. The dominant value was about 200 m. Thus, a typical event could have caused about 200 m of weakened area in rock mass around focal point where rupture processes had taken place.

The solution quality analysis of focal mechanisms calculated using full moment tensor inversion technique made us to choose L1 norm for presenting final results of mechanism solutions. This norm is characterized by lower sensitivity to data errors.

An analysis of fault planes orientations in the whole mine area as well as in its subregions does not lead to conclusions on any dominant fault plane orientation. It is unlikely that rupture processes of studied events are connected with any new activity on existing fault zones nor any known direction of cracks in the rockmass. The lack of dominant fault plane orientation may indicate that the studied events are mainly effects of post blasting relaxation and excavation of ores from beds. The studied period is too short to ensure us that the mentioned geological processes will not be initiated in the considered area of Rudna Copper Mine. It does, however, evidence that exploitation techniques had no detectable effect on tectonics.

In our opinion, a similar routine as described in our work, if periodically repeated, could provide additional information for mine engineers and can be used together with seismic event location and magnitude determination routines. The information about size and mechanisms of induced events can help in designing excavation works and blasting procedures in practice of stress release.

References

- Aki, K. and Richards, P. G. (1980) *Quantitative Seismology. Theory and Methods*, Freeman, San Francisco.
- Andrews, D. J. (1986) Objective determination of source parameters and similarity of earthquakes of different size. *Earthquake Source Mechanics* (S. Das, J. Boatwright, and C. H. Scholtz, eds.) Vol. 6, pp 259-267, Am. Geophys. Union, Washington, D.C.
- Hanks, T. C., and Kanamori, H. (1979) A moment magnitude scale. *J. Geophys. Res.* 84, 2348-2350.
- Madariaga, R. (1976) Dynamics of an expanding circular fault. *Bull. Seism. Soc. Am.* 66, 639-666.
- Snoke, J. A. (1987) Stable determination of (Brune) stress drops. *Bull. Seism. Soc. Am.* 64, 1295-1317.
- Wiejacz, P. (1991) Investigation of focal mechanisms of mine tremors by moment tensor inversion, Ph. D. thesis, Inst. Geophys., Pol. Acad. Sci., Warsaw (in Polish).

Geophysics in Mining and Environmental Protection

Idziak, A.F.; Dubiel, R. (Eds.)

2011, XII, 136 p., Hardcover

ISBN: 978-3-642-19096-4